Motor Condition Monitoring by Empirical Wavelet Transform

Levent Eren
Electrical and Electronics Engr.
Izmir University of Economics
Izmir, Turkey
levent.eren@ieu.edu.tr

Yalcin Cekic
Mechatronics Program
Bahcesehir University
Istanbul, TURKEY
yalcincekic@gmail.com

Michael J. Devaney
Electrical and Computer Engr.
University of Missouri
Columbia, USA
devaneym@missouri.edu

Abstract— **Bearing faults are by far the biggest single source of motor failures. Both fast Fourier (frequency based) and wavelet (time-scale based) transforms are used commonly in analyzing raw vibration or current data to detect bearing faults. A hybrid method, Empirical Wavelet Transform (EWT), is used in this study to provide better accuracy in detecting faults from bearing vibration data. In the proposed method, the raw vibration data is processed by fast Fourier transform. Then, the Fourier spectrum of the vibration signal is divided into segments adaptively with each segment containing part of the frequency band. Next, the wavelet transform is applied to all segments. Finally, inverse Fourier transform is utilized to obtain time domain signal with the frequency band of interest from EWT coefficients to detect bearing faults. The bearing fault related segments are identified by comparing rms values of healthy bearing vibration signal segments with the same segments of faulty bearing. The main advantage of the proposed method is the possibility of extracting the segments of interest from the original vibration data for determining both fault type and severity.**

Keywords— *empirical wavelet transform, Fourier transform, induction motors, bearing faults component,*

I. INTRODUCTION

Rolling element bearings are used widely in induction motor design and their failure is the single biggest cause for expensive production shutdowns in manufacturing industry [1]. Considering the heavy reliance on induction machines by the industry, there is a great amount of research effort directed towards monitoring of bearing health. Motor vibration and motor current analysis are commonly used noninvasive methods in bearing condition monitoring [2]. Time-domain [3], frequency-domain [8-11], enhanced frequency [12-15], and time–scale analysis [16-21] are four main areas where signal processing techniques are used in extracting information related to the bearing condition.

The use of Empirical Wavelet Transform (EWT) is proposed in this study to provide means for decomposing time domain vibration signal into segments with different frequency bandwidths. The fault related segments are determined by comparing the energy levels of healthy bearing vibration signal segments with the energy levels of faulty bearing segments. After determining the fault related segments, selected segments can be used to reconstruct the signal. Then, the reconstructed signal can be fed to an adaptive 1D Convolutional Neural Network (CNN) classifier for feature extraction and more accurate pattern recognition with a simple structure [22-23].

II. BEARING FAULTS

Bearing faults are mechanical faults accounting for most motor failures. Table I presents the surveys conducted by the Electric Power Research Institute (EPRI), which surveyed 6312 motors [24], and the survey conducted by the Motor Reliability Working Group of the IEEE-IAS, which surveyed 1141 motors [25].

Table 1 – Percentage of failure by component [26]

Failed Component	Percentage Failures (%)	
	IEE-IAS	**EPRI**
Bearings Related	44	41
Windings Related	26	36
Rotor Related	8	9
Others	22	14

It is obvious from the table that bearing related problems are the most common causes of motor failures.

Since bearing faults are the least expensive fault type to fix and at the same time the most difficult to detect, considerable amount of research is directed in this area. Typically, faulty bearings create characteristic frequencies in four different zones in the frequency spectrum: shaft speed zone, bearing defect frequency zone, bearing natural resonances zone, and high frequency zone [27].

The characteristic frequencies in the bearing defect frequency zone are determined from bearing geometry and shaft speed. The geometry of a typical ball bearing is depicted in Figure 1.
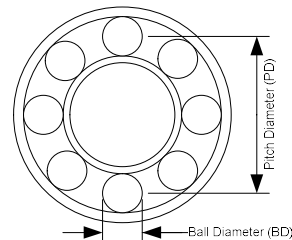

Figure 1, Ball bearing geometry

The characteristic vibration frequencies are calculated by the following equations [28].

The ball pass frequency outer (ring), *BPFO*, is given by

$$BPFO = \frac{n}{2}f_{rm}(1 - \frac{BD}{PD}cos\varphi) \qquad (1)$$

where the number of balls is *n*, the rotor speed in revolutions per second is *f_{rm}*, and the contact angle (zero for ball bearings) is *φ*.

The ball pass frequency inner, *BPFI*, is given by

$$BPFI = \frac{n}{2}f_{rm}(1 + \frac{BD}{PD}cos\varphi) \qquad (2)$$

The ball spin frequency, *BSF*, is given by

$$BSF = \frac{PD}{2BD}f_{rm}(1 - (\frac{BD}{PD})^2cos^2\varphi) \qquad (3)$$

The initial stage of a bearing fault is indicated by energy in both zones I and IV where the ladder zone contains high frequency components over 20 kHz. In the second stage of the fault, zone III with bearing natural frequencies will have some energy with increased energy levels in zone IV. The third stage is identified with bearing defect related frequencies becoming apparent in zone II and increased energy levels in other three zones. In the final stage, the bearing defect frequencies become more pronounced and their harmonics also show up in the frequency spectrum. The frequency content for all four stages of the bearing failure is depicted in figure 2.

This paper focuses on the detection of bearing fault frequencies in zone II and zone III for the final two stages of a bearing fault.

III. EMPIRICAL WAVELET TRANSFORM

In EWT, a signal is processed by fast Fourier transform (FFT) and the Fourier spectrum of the signal is divided into segments adaptively. Then, the scaling and wavelet functions are applied to the segments of interest.

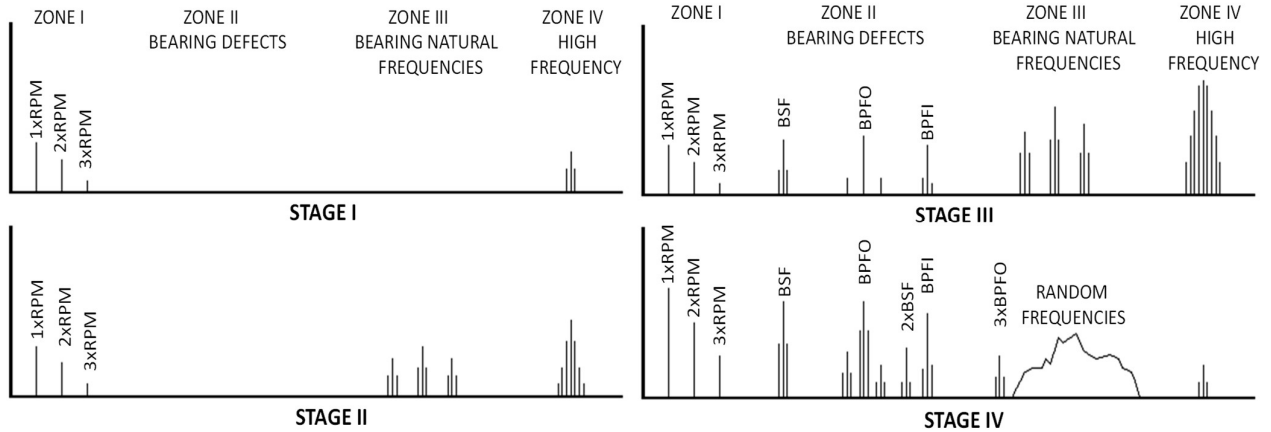$$X(w) = \sum_{n=0}^{\infty} x(n)e^{-inw} \qquad (4)$$

where w is defined in $[0,\pi]$.

Then, the spectrum is divided into N successive parts and w_l (l=1, 2, …,N) indicates the boundaries of the segment number. The empirical scaling, $\widehat{\emptyset}_l$, and wavelet, $\widehat{\psi}_l$, functions are defined by equations 5 and 6 respectively.

$$\widehat{\emptyset_l(w)} = \begin{cases} 1, & if \ |w| \leq (1-\gamma)w_l \quad (5) \\ cos\left[\frac{\pi}{2}\beta(\frac{1}{2\gamma w_l}(|w|-(1-\gamma)w_l)\right], & if \ (1-\gamma)w_l \leq |w| \leq (1+\gamma)w_l \\ 0, & otherwise \end{cases}$$

$$\widehat{\psi_l(w)} =$$

$$\begin{cases} 1, & if \ (1+\gamma)w_l \leq |w| \leq (1-\gamma)w_{l+1} \quad (6) \\ cos\left[\frac{\pi}{2}\beta(\frac{1}{2\gamma w_{l+1}}(|w|-(1-\gamma)w_{l+1})\right], & if \ (1-\gamma)w_{l+1} \leq |w| \leq (1+\gamma)w_{l+1} \\ sin\left[\frac{\pi}{2}\beta(\frac{1}{2\gamma w_l}(|w|-(1-\gamma)w_l)\right], & if \ (1-\gamma)w_l \leq |w| \leq (1+\gamma)w_l \\ 0, & otherwise \end{cases}$$

The detail and approximation coefficients are then given by

$$W_f^e(l,t) = <f,\psi_l> = F^{-1}\left[f(w)\widehat{\psi_l(w)}\right] \qquad (7)$$

and

$$W_f^e(0,t) = <f,\emptyset_l> = F^{-1}\left[f(w)\widehat{\emptyset_l(w)}\right] \qquad (8)$$

where F^{-1} denotes inverse Fourier transform. The empirical mode signal $f_k(t)$ of the vibration signal can be found by

$$f_0(t) = W_f^e(0,t) * \emptyset_l(t) \qquad (9)$$

and

$$f_k(t) = W_f^e(k,t) * \psi_k(t) \qquad (10)$$

The original vibration signal is then can be obtained by

$$f(t) = \sum_{k=0}^{L} f_k(t) \qquad (11)$$

Figure 2, Bearing damage stages

IV. Data Processing

IMS bearing dataset from NASA Prognostic Data Repository is used to test the performance of the proposed method [29]. In the test setup, the shaft is driven by a belt coupled to a motor at constant speed of 2000 rpm throughout the data collection process. The debris collected by magnetic plug is used to indicate the degradation in bearing health. In this case, the vibration data were collected at sampling rate of 20 kHz. The sampling was continuous but records of 20,480 data points were stored in a file once in every 5 or 10 minutes and stored in a file. Inner race, outer race, and roller element defects occurred in different bearings during data collection.

The empirical wavelet transform is applied to the data collected from accelerometer mounted on bearing 4 which develops an outer race defect. Rexnord ZA-2115 double row bearings with 16 rollers in each row are used in the test rig. Rexnord ZA-2115 double row bearings have a pitch diameter of 2.815 in., roller diameter of 0.331 in., and a tapered contact angle of 15.17°. Then, the equation 1 would yield the outer race fundamental vibration frequency of 236 Hz at rotational speed of 2000 rpm.

Here, the Fourier spectrum of the signal is split into bands adaptively based on energy content. EWT boundaries for a faulty bearing are depicted in figure 3.
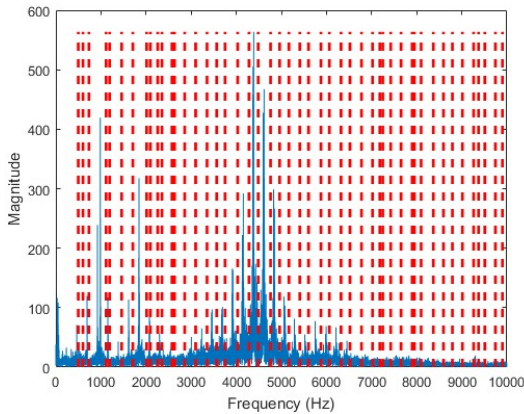

Figure 3, EWT boundaries of faulty bearing

After applying EWT and inverse Fourier transform, the contibution of each segment to the original time domain signal are determined. Calculating rms values for each segment and comparing rms values for faulty and healthy segments, the segments of interest can be selected.

Since we are interested only in two zones (II and III), two segments with biggest energy difference are selected from each zone. Segments three and five were selected for zone I whereas segments twentytwo and twentythree are chosen for zone III. The corresponding frequency bands are 600-734 Hz, 1114-1191 Hz, 4485-4759 Hz, and 4759-4961 Hz respectively. The contribution of segment five (1114-1191 Hz) in time domain for both cases are depicted in figure 4. The segments and segment sizes are determined using faulty set of data.
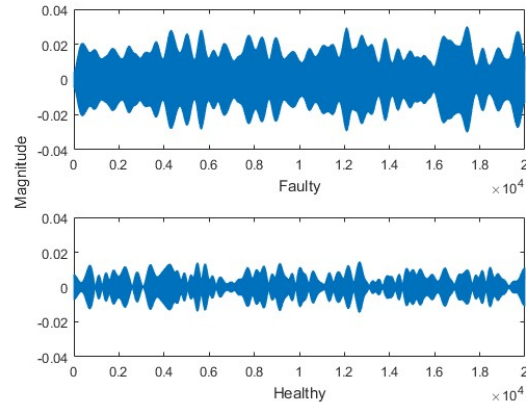

Figure 4, Time domain contribution of segment five

The Fourier spectrum for both cases are plotted in figure 5 to verify that the increase in rms levels of segment five is due to bearing fault related frequencies. Here, the peak is around 1180 Hz, the fifth harmonic of the outer race defect frequency, for the faulty case.
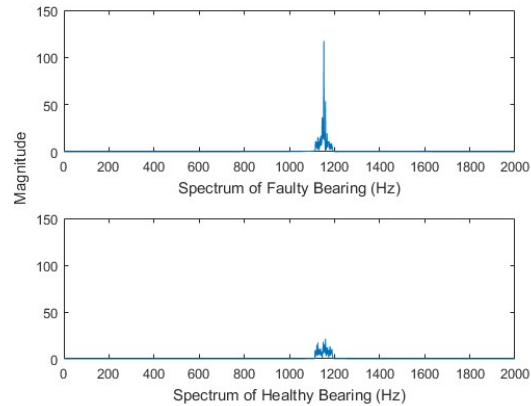

Figure 5, Frequency domain contribution of segment five

Similarly, contribution of segment twentytwo (4485-4759 Hz) in time domain for both cases are depicted in figure 6.
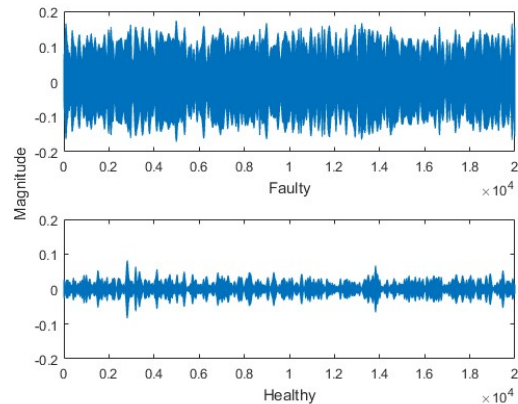

Figure 6, Time domain contribution of segment twentytwo

The final stage of the analysis involves taking inverse Fourier transform of the empirical wavelet coefficients for the segments of the interest and calculating rms values of resulting signals to detect bearing faults. The rms values of segments three, five, twentytwo, and twentythree are given in table 2 for both healthy and faulty bearing cases.

Table 2 – Rms values of selected segments

Segment / Zone	RMS Values	
	Healthy	Faulty
Segment 3 / Zone II	0.0074	0.0138
Segment 5 / Zone II	0.0054	0.0126
Segment 22 / Zone III	0.0172	0.0803
Segment 23 / Zone III	0.0131	0.0478

There is increase in energy levels in all segments for the faulty case compared to the energy levels of the healthy case. Usually about 50% increase in energy levels of healthy baseline data can signal fault conditions. The considerable amount of increase in rms values for segments 22 and 23 indicate advanced stages of fault detected.

V. CONCLUSION

Empirical Wavelet Transform (EWT), is used in this study to provide better accuracy in detecting faults from raw vibration data. The main advantage of the proposed method is the possibility of extracting only the segments of interest from the original vibration signal. In the proposed method, the raw vibration data is processed by fast Fourier transform for both faulty and healthy bearings. Then, the Fourier spectrum of the vibration signal is divided into segments adaptively. Segments three, five, twentytwo and twentythree are selected for analysis since they correspond to zone II and zone III frequencies. Next, the wavelet transform is applied to all segments of interest and inverse Fourier transform is utilized to obtain time domain contributions of those segments. Finally, rms values of time domain signals are computed to find increases due to bearing faults. The results showed that the fault condition can be detected by the proposed method. Furthermore, the rms values of the selected segments can be used as features for neural networks or time domain components of segments may be fed directly to 1D CNN for detection and classification.

The segment sizes and locations may depend on both the fault type and the bearing geometry. The optimal set of segments and segment sizes may be determined if bearing geometry is available. Our future work will focus on determining such a set of segments with fixed sizes.

REFERENCES

[1] H. A. Toliyat, S. Nandi, S. Choi, and H. Meshgin-Kelk, Electric Machines:Modeling, ConditionMonitoring, and Fault Diagnosis, CRC Press, 2012.

[2] R. B. Randall, Vibration-Based ConditionMonitoring: Industrial,Aerospace and Automotive Applications, John Wiley & Sons,Chichester, UK, 2011.

[3] H. Henao, G.-A. Capolino, M. Fernandez-Cabanas et al., "Trends in fault diagnosis for electrical machines: a review of diagnostic techniques," IEEE Industrial Electronics Magazine, vol. 8, no. 2, pp. 31–42, 2014.

[4] W. Zhou, T. G. Habetler, and R. G. Harley, "Bearing fault detection via stator current noise cancellation and statistical control," IEEE Transactions on Industrial Electronics, vol. 55, no. 12, pp. 4260–4269, 2008.

[5] P. D. McFadden and J. D. Smith, "Model for the vibration produced by a single point defect in a rolling element bearing," Journal of Sound and Vibration, vol. 96, no. 1, pp. 69-82, 1984.

[6] Y.-T. Su and S.-J. Lin, "On initial fault detection of a tapered roller bearing: Frequency domain analysis," Journal of Sound and Vibration, vol. 155, no. 1, pp. 75-84, 1992.

[7] R. R. Schoen, T. G. Habetler, F. Kamran, and R. G. Bartheld, "Motor bearing damage detection using stator current monitoring," IEEE Transactions on Industry Applications, vol. 31, no. 6, pp. 1274-1279, 1995.

[8] G. B. Kliman, W. J. Premerlani, B. Yazici, R. A. Koegl, and J. Mazereeuw, "Sensorless, online motor diagnostics," IEEE Computer Applications in Power, vol. 10, no. 2, pp. 39-43, 1997.

[9] J. Pons-Llinares, J. A. Antonino-Daviu, M. Riera-Guasp, S. B. Lee, T.-J. Kang, and C. Yang, "Advanced induction motor rotor fault diagnosis via continuous and discrete time-frequency tools," IEEE Transactions on Industrial Electronics, vol. 62, no. 3, pp. 1791-1802, 2015.

[10] N. Arthur and J. Penman, "Induction machine condition monitoring with higher order spectra," IEEE Transactions on Industrial Electronics, vol. 47, no. 5, pp. 1031-1041, 2000.

[11] M. E. H. Benbouzid, M. Vieira, and C. Theys, "Induction motors' faults detection and localization using stator current advanced signal processing techniques," IEEE Transactions on Power Electronics, vol. 14, no. 1, pp. 14-22, 1999.

[12] D. Z. Li, W. Wang, and F. Ismail, "An enhanced bispectrum technique with auxiliary frequency injection for induction motor health condition monitoring," IEEE Transactions on Instrumentation and Measurement, vol. 64, no. 10, pp. 2679- 2687, 2015.

[13] L. Eren and M. J. Devaney, "Bearing damage detection via wavelet packet decomposition of the stator current," IEEE Transactions on Instrumentation and Measurement, vol. 53, no. 2, pp. 431-436, 2004.

[14] Z. Ye, B. Wu, and A. Sadeghian, "Current signature analysis of induction motor mechanical faults by wavelet packet decomposition," IEEE Transactions on Industrial Electronics, vol. 50, no. 6, pp. 1217-1228, 2003.

[15] R. Yan, R. X. Gao, and X.Chen, "Wavelets for fault diagnosis of rotary machines: a review with applications," Signal Processing, vol. 96, pp. 1-15, 2014.

[16] S. Prabhakar, A. R. Mohanty, and A. S. Sekhar, "Application of discrete wavelet transform for detection of ball bearing race faults," Tribology International, vol. 35, no. 12, pp. 793-800, 2002.

[17] X. Zhang, J. Zhou, "Multi-fault diagnosis for rolling element bearings based on ensemble empirical mode decomposition and optimized support vector machines," Mech. Syst. Signal Process., vol. 41, pp. 127-140, 2013.

[18] J. Gilles, "Empirical wavelet transform," IEEE Trans. Signal Process, vol. 61, no. 16, pp. 3999-4010, 2013.

[19] H. R. Cao, F. Fan, and K. Zhou, Z. J. He, "Wheel-bearing fault diagnosis of trains using empirical wavelet transform," Measurement, vol. 82, pp. 439-449, 2016.

[20] J. Chen, J. Pan, Z. Li, Y. Zi, and X. Chen, "Generator bearing fault diagnosis for wind turbine via empirical wavelet transform using measured vibration signals," Renewable Energy, vol. 89, pp. 80-92, 2016.

[21] D. Wang, Y. Zhao, C. Yi, K.L. Tsui, and J. Lin, "Sparsity guided empirical wavelet transform for fault diagnosis of rolling element bearings," Mechanical Systems and Signal Processing, vol. 101, pp. 292-308, 2018.

[22] T. Ince, S. Kiranyaz, L. Eren, M. Askar, and M. Gabbouj, "Real-time motor fault detection by 1D convolutional neural networks." IEEE Transactions Industrial Electronics, vol. 63, pp. 7067-7075. 2016.

[23] L. Eren, "Bearing fault detection by one-dimensional convolutional neural networks," Mathematical Problems in Engineering, pp. 1-9, 2017.

[24] I. C. Report, "Report of large motor reliability survey of industrial and commercial installation, Part I and Part II," IEEE Transactions on Industry Applications, vol. 21, pp. 853-872, 1985.

[25] P. F. Albrecht, J. C. Appiarius, and D. K. Sharma, "Assessment of the reliability of motors in utility applications-Updated," IEEE Transactions on Energy Conversion, vol. 1, pp. 39-46, 1986.

[26] A. M. Da Silva, "Induction Motor Fault Diagnostic and Monitoring Methods", A Thesis submitted to the Faculty of the Graduate School, Marquette University, Milwaukee, Wisconsin, May 2006.

[27] STI Field Application Note, Rolling Element Bearings, REB, Sales Technology, League City, Tex, USA, 2012.

[28] V. Wowk, Machinery Vibration, Measurement and Analysis, McGraw-Hill, 1991.

[29] J. Lee, H. Qiu, G. Yu, and J. Lin, Rexnord Technical Services: Bearing Data Set, 2007.